Speckles Statistics and Decorrelation Effects
in Complex ABCD Optical Systems

Prepared by

H. T. YURA
The Aerospace Corporation
Los Angeles, CA 90009

S. G. HANSON
Risø National Laboratory
Roskilde, Denmark

T. P. GRUM
University of Copenhagen
Copenhagen Ø, Denmark

15 December 1992

Prepared for

SPACE AND MISSILE SYSTEMS CENTER
AIR FORCE MATERIEL COMMAND
Los Angeles Air Force Base
P. O. Box 92960
Los Angeles, CA 90009-2960

Programs Group

DTIC
ELECTE
AUG 1 1 1993
S
C
D

THE AEROSPACE CORPORATION
El Segundo, California

93-18485

93 8

This report has been reviewed by the Public Affairs Office (PAS) and is releasable to the National Technical Information Service (NTIS). At NTIS, it will be available to the general public, including foreign nationals.

This technical report has been reviewed and is approved for publication. Publication of this report does not constitute Air Force approval of the report's findings or conclusions. It is published only for the exchange and stimulation of ideas.

ALFRED DUENAS, Capt, USAF
Sensor Acquisition Manager
DSP

WM KYLE SNEDDON, Capt, USAF
Industrial and International Division
Plans and Programs Directorate

REPORT DOCUMENTATION PAGE

1a. REPORT SECURITY CLASSIFICATION Unclassified	1b. RESTRICTIVE MARKINGS
2a. SECURITY CLASSIFICATION AUTHORITY	3. DISTRIBUTION/AVAILABILITY OF REPORT
2b. DECLASSIFICATION/DOWNGRADING SCHEDULE	Approved for public release; distribution unlimited
4. PERFORMING ORGANIZATION REPORT NUMBER(S) TR-92(2409)-3	5. MONITORING ORGANIZATION REPORT NUMBER(S) SMC-TR-93-35

6a. NAME OF PERFORMING ORGANIZATION The Aerospace Corporation Technology Operations	6b. OFFICE SYMBOL (If applicable)	7a. NAME OF MONITORING ORGANIZATION Space and Missile Systems Center
6c. ADDRESS (City, State, and ZIP Code) El Segundo, CA 90245-4691		7b. ADDRESS (City, State, and ZIP Code) Los Angeles Air Force Base Los Angeles, CA 90009-2960
8a. NAME OF FUNDING/SPONSORING ORGANIZATION	8b. OFFICE SYMBOL (If applicable)	9. PROCUREMENT INSTRUMENT IDENTIFICATION NUMBER F04701-88-C-0089

8c. ADDRESS (City, State, and ZIP Code)	10. SOURCE OF FUNDING NUMBERS			
	PROGRAM ELEMENT NO.	PROJECT NO.	TASK NO.	WORK UNIT ACCESSION NO.

11. TITLE (Include Security Classification)

Speckles Statistics and Decorrelaton Effects in Complex ABCD Optical Systems

12. PERSONAL AUTHOR(S)
Yura, H. T.; Hanson, S. G.; and Grum, T. P.

13a. TYPE OF REPORT	13b. TIME COVERED FROM _____ TO _____	14. DATE OF REPORT (Year, Month, Day) 1992 December 15	15. PAGE COUNT 35

16. SUPPLEMENTARY NOTATION

17. COSATI CODES			18. SUBJECT TERMS (Continue on reverse if necessary and identify by block number)
FIELD	GROUP	SUB-GROUP	ABCD Matrix Methods, Interferometry, Photon Statistics Speckle

19. ABSTRACT (Continue on reverse if necessary and identify by block number)

The mean, variance and correlation function of the intensity pattern resulting from an incoherent source that has propagated through a complex ABCD optical system is derived. The number of speckle correlation cells (or modes) within an effective measurement area is presented and discussed. Optical field decorrelation effects regarding secondary fringe formation in phase shifting speckle interferometry is discussed. In particular, the correlation coefficient resulting from load-induced object tilt, in-plane translations, and displacements parallel to the optic axis as a function of the number of modes propagating through the optical system is described and discussed.

20. DISTRIBUTION/AVAILABILITY OF ABSTRACT [X] UNCLASSIFIED/UNLIMITED ☐ SAME AS RPT. ☐ DTIC USERS	21. ABSTRACT SECURITY CLASSIFICATION Unclassified	
22a. NAME OF RESPONSIBLE INDIVIDUAL	22b. TELEPHONE (Include Area Code)	22c. OFFICE SYMBOL

DD FORM 1473, 84 MAR   83 APR edition may be used until exhausted. All other editions are obsolete.

PREFACE

The present work was partly supported by The Technical Research Council in Denmark.

DTIC QUALITY INSPECTED 3

Accesion For		
NTIS CRA&I	☑	
DTIC TAB	☐	
Unannounced	☐	
Justification		
By		
Distribution /		
Availability Codes		
Dist	Avail and / or Special	
A-1		

1

CONTENTS

FIGURES

TABLE

1. Introduction

Complex ABCD ray matrix techniques combined with the paraxial approximation of the Huygens-Fresnel formulation of wave optics is a useful tool in analyzing analytically the performance of a rather general class of optical systems[1]. This method expresses the complex optical field in the observation (or output) plane as an integral over an initial (or input) plane of the given source distribution multiplied by a propagation kernel, which is a function of the ABCD matrix elements of the complete optical system between the input and output plane and properties of the intervening medium which the light propagates through. Thus, for example, the effects of a random medium (e.g., turbulence) and incoherent sources can be described by using this technique [2,3]. By employing such methods one is able in a straight forward manner to obtain expressions for all the statistical correlation functions that pertain to the optical system, source distribution and intervening media under consideration.

The use of complex ABCD matrix elements permits modelling of limiting apertures (e.g., thin lens, field stops, and finite sized measurement apertures) as soft (i.e., Gaussian) apertures. In many applications (e.g., imaging and Fourier transform systems) such modelling yields useful engineering analytical approximations to system performance that can be used for designing, sizing and scaling of optical systems. In addition, the results can generally be cast in a physically intuitive form, where, for example, the effects of geometric optics and diffraction are readily apparent.

5

In this paper we consider homogeneous media and derive in sec. 2 expressions for the mean, variance and corresponding correlation function of the irradiance distribution resulting from an incoherent source that has propagated through a complex (axially symmetric) ABCD optical system. In particular, we obtain a general expression for the mutual coherence function which can be regarded as a generalization of the van Cittert-Zernike theorem to complex paraxial ABCD systems. We also derive an expression that relates the number of speckle correlation cells contained within a measurement area to the parameters of the ABCD system. In particular, an expression for the maximum number of independent intensity measurements that the optical system allows is obtained.

In sec. 3 we consider the effects of wave front decorrelation on fringe formation in speckle interferometric systems. Such interferometers brings about a real-time technique for non-destructive measurements of deformations and contours of objects that scatter laser light diffusively. To make measurements using double exposure speckle interferometry, a speckle-pattern exposure of the object is taken in one position. The object is then deformed (i.e., put under load) and another exposure is taken. These two speckle patterns are subtracted, and their difference is squared to obtain speckle correlation fringes that correspond to the objects movement and deformation[4]. Here we examine the effects of load induced object tilt around an in-plane axis, in-plane and out of plane object displacement on decorrelation of the interferograms operating in the subtraction mode.

Decorrelation and the corresponding fringe visibility in image-plane electronic speckle-pattern correlation interferometers has been considered recently by Owner-Petersen[5]. However, it can be shown (see Appendix) that

6

the correlation function derived in Ref. 5 is valid only for the case where the number of independent speckle modes N is much larger that unity (i.e., N → ∞). Here we derive expression for the correlation function for both an arbitrary ABCD system and finite N. In particular it is shown that as N → 1, the correlation coefficient is equal to unity. That is, in this limit the performance of phase difference speckle interferometers do not degrade under load induced object deformations.

2. Intensity Statistics for Incoherent Sources

We consider a completely incoherent, finite sized, quasi-monochromatic, polarized optical source located in an input plane and assume that a paraxial optical system, characterized by a complex ABCD ray matrix, occupies the space between the primary source and an observation plane. For definiteness, we consider an axially symmetric paraxial optical system that includes a radially increasing optical amplitude loss with respect to the optic axis. In particular, we consider a general paraxial system which includes a Gaussian variation in amplitude transmission across the axis. It has been shown that such systems can be described by a complex valued ABCD ray matrix [1,2].

By using a Huygens-Fresnel integral formulation, whose propagation kernel is a function of the system ABCD matrix elements, one can express the complex optical field in the observation plane of an axially symmetric system where the input and output planes are in the same medium, as

$$U(\underline{p}) = \left[-\frac{ikt_o}{2\pi B}\right] exp(-ikL)\int d^2r \ U_s(\underline{r})$$

7

$$\times \, exp\left[-\frac{ik}{2B}\left(Dp^2 - 2\underline{r}\cdot\underline{p} + Ar^2\right)\right], \tag{1}$$

where k is the optical wave number in free space, L is the optical distance along the z-axis, $\underline{r}$ and $\underline{p}$ are coordinate vectors transverse to the z-axis in the source and observation plane, respectively, t_o is the on-axis transmission amplitude factor and A,B, and D are the overall complex ray matrix elements for the system under consideration from the input to the output plane. Without loss of generality we can assume that $t_o = 1$.

We now apply Eq. (1) to the special case where the source is incoherent and obtain general expressions for the mean and second moment of the observed intensity. In any experimental measurement of the intensity one employs detectors of finite size. Following Goodman [6], the instantaneous measured intensity is expressed as

$$I_M = \frac{1}{S}\int d^2p \, W(\underline{p}) \, I(\underline{p}), \tag{2}$$

where $\underline{p} = (p_x, p_y)$, $I(\underline{p}) = |U(\underline{p})|^2$, $W(\underline{p})$ is a real and positive measurement aperture weighting function, and $S = \int W(\underline{p})d^2p$. Due to the presence of $W(\underline{p})$ the integration indicated in the above can be considered to be over the entire observation plane.

From Eqs. (1) and (2) the mean measured intensity can be expressed as

$$\langle I_M \rangle = \frac{1}{S}\int d^2p \, W(\underline{p}) \, \langle I(\underline{p}) \rangle \tag{3}$$

8

where

$$\langle I(\underline{p}) \rangle = \frac{1}{|B|^2} \, exp\left[k \ Im(D/B)p^2\right] \int d^2r \ I_s(\underline{r}) \ exp \ [-2k \ Im(1/B)\underline{p}\cdot\underline{r}]$$

$$\times \ exp[k \ Im(A/B)r^2], \tag{4}$$

where Im denotes the imaginary part, and the angular brackets indicate on ensemble average over the statistics of the source. In obtaining Eq. (4) we used the relation, valid for an incoherent source radiating into a half-space, $(k^2/2\pi)\langle U_s(\underline{r}_1)U_s^*(\underline{r}_2)\rangle = I_s[(r_1+r_2)/2]\delta(\underline{r}_1-\underline{r}_2)$, where $\delta(\underline{r})$ is the two-dimensional Dirac delta function and I_s is the radiated power per unit area of the source. By considering the field of a point source located at a point $\underline{r}$ in the input plane, it can be shown for a system with no gain and a radially increasing loss across the optic axis that both $Im(A/B)$ and $Im(D/B)$ are less than or equal to zero. As a result, the integrals in Eqs. (3) and (4) are finite for any practical source distribution of interest.

In a similar manner, the mean square of the measured intensity can be expressed as

$$\langle I_M^2 \rangle = \frac{1}{S^2} \int d^2P_1 \int d^2P_2 \ W(\underline{p}_1) \ W(\underline{p}_2)\langle I(\underline{p}_1)I(\underline{p}_2)\rangle \tag{5}$$

Assuming circular complex Gaussian statistics for the underlying source field, it can be shown that the intensity autocorrelation function can be expressed as [6]

$$\langle I(\underline{p}_1)I(\underline{p}_2)\rangle = \langle I(\underline{p}_1)\rangle\langle I(\underline{p}_2)\rangle\left[1 + |\gamma(\underline{p}_1,\underline{p}_2)|^2\right] \tag{6}$$

9

where

$$|\gamma(\underline{p}_1,\underline{p}_2)| = \frac{|\Gamma(\underline{p}_1,\underline{p}_2)|}{[<I(\underline{p}_1)><I(\underline{p}_2)>]^{1/2}} \tag{7}$$

is the absolute magnitude of the complex degree of coherence. The quantity Γ is the mutual coherence function of the field in the observation plane and is given by

$$\Gamma(\underline{p}_1,\underline{p}_2) = <U(\underline{p}_1)\,U^*(\underline{p}_2)>$$

$$= |\frac{-ik}{2\pi B}|^2\,exp\left[-\frac{ik}{2}\left(\frac{D}{B}\,p_1^2 - \frac{D^*}{B^*}\,p_2^2\right)\right]\int d^2r I_s(\underline{r})$$

$$\times\,exp\left[ik\underline{r}\cdot\left(\frac{\underline{p}_1}{B} - \frac{\underline{p}_2}{B^*}\right)\right]\,exp\left[kIm(A/B)r^2\right] \tag{8}$$

Equation 8 is the generalization of the mutual coherence function for propagation in a homogeneous medium, given by Eq. (20) of Ref. 7 chapter 10.4.2 , to complex ABCD optical systems. Thus, Eq. (8) can be regarded as a generalization of the van Cittert-Zernike theorem to complex paraxial ABCD optical systems.

Examination of Eq. (8) reveals that the statistics of intensity for a complex ABCD system are not stationary but rather depend on absolute position $\underline{p}_1$ and $\underline{p}_2$. For a given circularly symmetric ABCD system containing soft apertures the mean irradiance and mutual coherence function is given by Eqs. (4) and (8), respectively. The corresponding measured mean and mean square intensity are given by Eqs. (3) and (5). Due to the assumption of an underlying Gaussian statistics for the complex field all higher moments of the intensity

can be expressed by suitable products of the corresponding first and second moments.

Another quantity of interest is the number of speckle correlation cells N within the measurement aperture. Following Goodman[6] this quantity is given by

$$N = \frac{\langle I_M \rangle^2}{Var[I_M]}$$

$$= \frac{\langle I_M \rangle^2}{\langle I_M^2 \rangle - \langle I_M \rangle^2} \tag{9}$$

Substituting Eqs. (3) and (5) into Eq. (9) yields

$$N = \frac{[\int W(\underline{p}) \langle I(\underline{p}) \rangle d^2 p]^2}{\int\int W(\underline{p}_1) W(\underline{p}_2) \langle I(\underline{p}_1) \rangle \langle I(\underline{p}_2) \rangle |\gamma(\underline{p}_1, \underline{p}_2)|^2 d^2 p_1 d^2 p_2} \tag{10}$$

where $\langle I(\underline{p}) \rangle$ and $|\gamma(\underline{p}_1, \underline{p}_2)|$ are given by Eqs. (4) and (7), respectively.

In order to proceed we specialize to the case where the intensity distribution of the source is of gaussian shape given by $I_s(r) = I_o exp(-2r^2/r_s^2)$. In addition we consider the situation where the beam spot size in the observation plane is much smaller than the extent of the measurement aperture; that is, we assume W = constant for $I(\underline{p}) \neq 0$. Note, if the measurement aperture is characterized by a Gaussian shaped weighting function, it can be formally included directly in the ABCD matrix elements as being the last optical element, immediately in front of the observation plane.

Upon performing the integration indicated in Eq. (8) it can be shown that the mutual coherence function is given by

$$\Gamma(\rho_1, \rho_2) = \frac{2I_o}{k^2 \rho_o^2} \, \rho_o \, \exp\left[- \frac{(\rho_1 - \rho_2)^2}{\rho_o^2}\right] \exp\left[- \frac{(\rho_1^2 + \rho_2^2)}{\omega^2}\right] \cdot \tag{11}$$

$$\exp\left[i \left\{\frac{Im(B)^2}{\rho_o^2 |B|^2} - \frac{k}{2} \, Re(D/B)\right\} (\rho_1^2 - \rho_2^2)\right]$$

where

$$\rho_o^2 = \frac{8|B|^2}{k^2 r_s^2} + \frac{4}{k} \, Im(BA^*) \tag{12}$$

and

$$\omega^2 = \rho_o^2 \left[\frac{|B|^2}{2(Im(BD^*)Im(BA^*) \, - \, (ImB)^2) + \frac{4|B|^2}{k^2 r_s^2} Im(BD^*)}\right] \tag{13}$$

The corresponding expression for the beam intensity profile and the magnitude of the degree of coherence are given by

$$\langle I(\rho)\rangle = \frac{2I_o}{k^2 \rho_o^2} \, \exp\left[- 2\rho^2/\omega^2\right] \tag{14}$$

and

$$|\gamma| = \exp\left[- (\rho_1 - \rho_2)^2/\rho_o^2\right] \tag{15}$$

The quantity ρ_o is a measure of the lateral extent of the region in the observation plane where the optical field is correlated (and is hence a measure of the mean speckle size) while the quantity ω is a measure of the beam intensity spot size. For a given ABCD system, these quantities can be obtained directly from Eqs. (12) and (13).

The number of speckle correlation cells within the beam, as obtained from Eq. (10), is given by

$$N = 1 + 2 \frac{\omega^2}{\rho_o^2} \tag{16}$$

As an illustrative ABCD system we consider an optical system that images a Gaussian shaped incoherent source onto an observation plane. A positive thin lens of Gaussian transmission radius σ is located a distance L_1 to the right of the source. At a further distance L_2 a Gaussian shaped aperture (i.e., a measurement aperture) of radius σ_a is immediately to the left of the image plane. The appropriate ray matrix elements can be calculated in a straighforward manner with the result that

$$A = - \frac{L_2}{L_1} - \frac{2i\,L_2}{k\sigma^2} \tag{17a}$$

$$B = - \frac{2i\,L_1 L_2}{k\sigma^2} \tag{17b}$$

and

$$D = - \frac{L_1}{L_2} - \frac{2i\,L_1}{k\sigma^2} \tag{17c}$$

13

Substituting Eqs. (17) into Eqs. (12) and (13) yields that

$$\rho_o^2 = \frac{8L_2^2}{k^2\sigma^2}\left(1 + \frac{4L_1^2}{k^2 r_s^2 \sigma^2}\right) \tag{18}$$

and

$$\omega^2 = \left[\frac{1}{\sigma_a^2} + \frac{1}{\omega_\infty^2}\right]^{-1} \tag{19}$$

where

$$\omega_\infty = \left[\left(\frac{L_2}{L_1}\right)^2 r_s^2 + \left(\frac{2L_2}{k\sigma}\right)^2\right]^{1/2} \tag{20}$$

is the spot size in the observation plane (i.e., image plane) for an infinite measurement aperture radius. Examination of Eq. (20) reveals that there are two contributions to ω_∞; the first term under is a geometric magnification of the source size and the second term represents the effects of diffraction from the finite size of the imaging lens.

Equation (19) gives the effect of a finite measurement aperture on the image size. As expected, for values of σ_a much larger (smaller) than ω_∞ the resulting image size is given by ω_∞ (σ_a). On the other hand the coherence length ρ_o is independent of σ_a, as it should.

The number of correlation cells contained in the imaged spot is obtained from Eqs. (16), (18), and (19) as

14

$$N = 1 + \frac{2\,(\sigma_{a}/\rho_{0})^{2}}{1 + (\sigma_{a}/\omega_{\infty})^{2}} \qquad (21)$$

and is plotted in Fig. 1 as a function of σ_{a}/ρ_{0} (i.e., the ratio of the measurement aperture to the coherence length) for various values of $\sigma_{a}/\omega_{\infty}$. For fixed σ_{a}, the number of correlation cells increase for decreasing values of ρ_{0}, the corresponding increase being progressively less for increasing values of $\sigma_{a}/\omega_{\infty}$.

As a further illustrative example, we consider a Fourier transform geometry with a finite sized thin transform lens of positive focal length f and gaussian radius σ. As in the previous example a gaussian shaped measurement aperture of radius σ_{a} is assumed to be just in front of the Fourier plane. In this case the relevant matrix elements are given by

$$A = -\frac{2if}{k\sigma^{2}} \qquad (22a)$$

$$B = f - \frac{2f^{2}i}{k\sigma^{2}} \qquad (22b)$$

and

$$D = -\frac{4f^{2}}{(k\sigma\sigma_{a})^{2}} - \frac{2fi}{k}\left[\frac{1}{\sigma^{2}} + \frac{1}{\sigma_{a}^{2}}\right] \qquad (22c)$$

Substituting Eqs. (22) into Eqs. (12) and (13) yields that

$$\rho_{0}^{2} = \frac{8f^{2}}{k^{2}r_{a}^{2}}\left[1 + \left(\frac{2f}{k\sigma^{2}}\right)^{2}\right] + \frac{8f^{2}}{k^{2}\sigma^{2}} \qquad (23)$$

and ω^{2}, the spot size in the Fourier plane, is given by Eq. (19) where
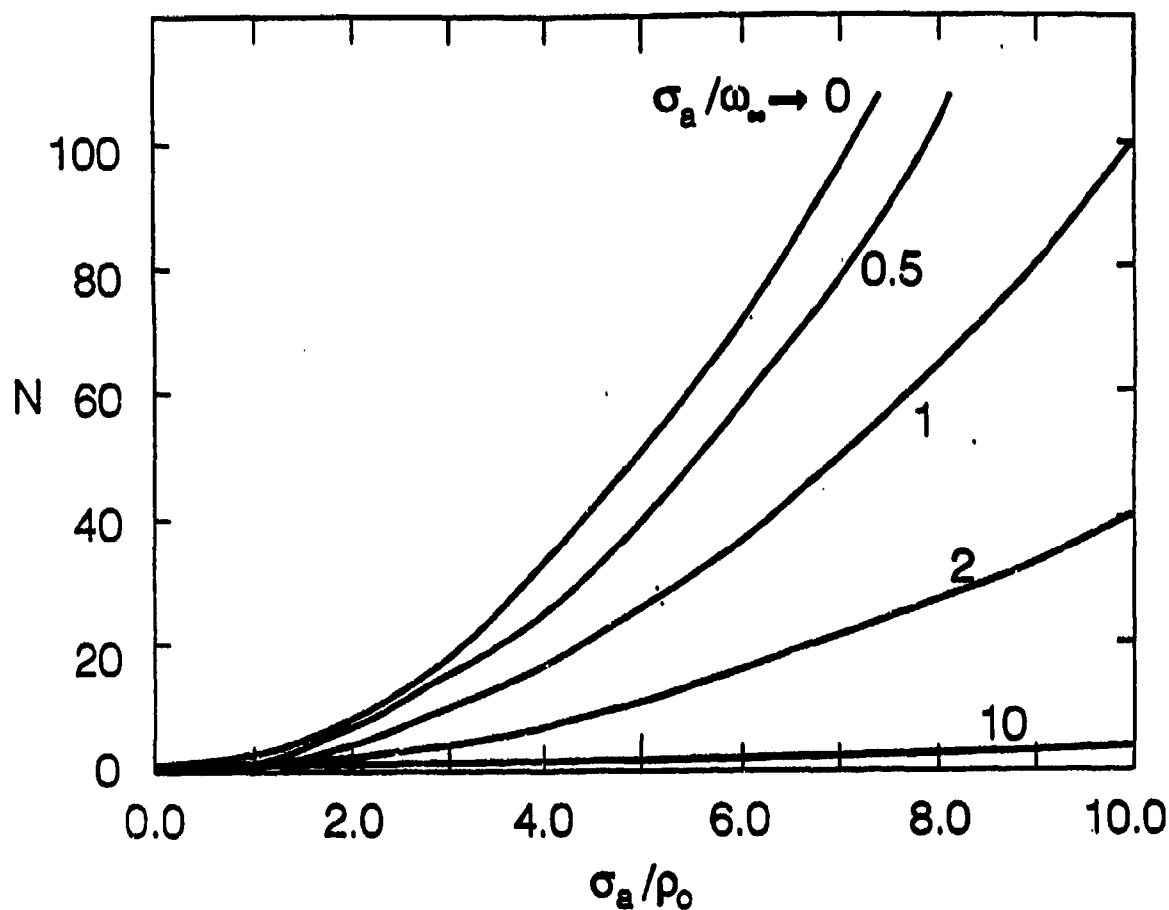
Figure 1. The number of intensity correlation cells for imaging and Fourier transform geometries contained in the measurement aperture as function of the "aperture radius:" (normalized to the lateral coherence length in the observation plane) for various values of σ_a/ω_∞. For the imaging and Fourier transform geometries, the quantities ρ_0 and ω_∞ are given by Eqs. (18) and (19), and Eqs. (23) and (24), respectively.

$$\omega_{\infty} = \left[r_s^2 + \sigma^2 + \left(\frac{2f}{k\sigma} \right)^2 \right]^{1/2} \tag{24}$$

The number of correlation cells contained in the measurement aperture is formally the same as Eq. (21), with ρ_0 and ω_∞ given by Eqs. (23) and (24), respectively.

Finally, consider the case of an extended incoherent source (i.e., $r_o \to \infty$). Of particular interest is the number of correlation cells N. For $r_o \to \infty$, N is independent of the source and depends on the wavelength and properties of the optical system only. Since the underlying probability density for the complex field has been assumed Gaussian, N also gives the number of statistically independent speckle modes. For $r_s \to \infty$, N can be interpreted as the maximum number of independent intensity measurements that the optical system allows. For an arbitrary complex ABCD system the maximum number of independent intensity measurements allowable is given by

$$N_{max} = 1 + \frac{|B|^2}{Im(BA^*)Im(BD^*) - (ImB)^2} \tag{25}$$

Note, for a point source (i.e., $r_s \to 0$) the corresponding number of modes, as expected, is equal to unity. For the imaging and Fourier transform geometries N_{max} is given by

$$N_{max} = 1 + \left(\frac{k\sigma \, \sigma_s}{2d} \right)^2, \tag{25}$$

where $d = L_2$ and f for the imaging and Fourier transform geometry, respectively.

17

3. Correlation Functions in Phase Shifting Interferometers

A basic characteristic of phase shifting interferometer operating in the subtraction mode, being electronic or holographic, is the formation of secondary fringes by taking the difference and squaring the two primary interferograms, before and after loading[4]. Then the ensemble averaged secondary fringe pattern is obtained as

$$< (I_a - I_b)^2 > = <I_a^2> + <I_b^2> - 2<I_a I_b>, \qquad (26)$$

where, for notational convenience, we have suppressed the functional dependence on observation plane coordinates $\underline{p}$, the subscripts b and a denote before and after loading, and angular brackets denote the ensemble average (i.e., over all possible realizations of the source distribution of scattered light). Now each of the interferograms I_a and I_b, found from two primary wave fronts U_1 and U_2, is given by

$$I = |U_1 + U_2|^2 = I_1 + I_2 + 2Re[U_1 U_2^*] \qquad (27)$$

where $I_{1,2} = |U_{1,2}|^2$. Assuming that U_1 and U_2 are stochastically independent and that the intensity of a speckle pattern obeys negative exponential statistics, M. Owner-Petersen has calculated the secondary fringe pattern and corresponding visibility V of the correlation fringes for the cases where U_1 is speckled and U_2 may be speckled. The situation where U_1 and U_2 are speckled and decorrelate under load is relevant both to the in-plane displacement sensitive interferometer and to the out-of-plane gradient interferometer, where both the primary wavefronts U_1 and U_2 are scattered from the surface under test. The situation when only U_1 decorrelates under load is relevant to the out-of-plane displacement sensitive interferometer, where U_2 represents a deterministic reference wave. Central to the quality of

19

the secondary fringes in the various interferometers is the correlation coefficient of the complex fields in the observation plane before and after loading. This quantity is defined as

$$\gamma = \frac{\langle U_b U_a^* \rangle}{\sqrt{\langle |U_a|^2 \rangle} \; \sqrt{\langle |U_b|^2 \rangle}} \qquad (28)$$

where it is assumed that both U_1 and U_2 have the same correlation function[5]. In general γ is complex with $0 \leq |\gamma| \leq 1$. Thus the effects of decorrelation are a distortion and corresponding reduction of fringe visibility in the observation plane (e.g., $V \to 0$ as $|\gamma| \to 0$). Owner-Petersen derives an explicit expression for the decorrelation coefficient in a direct image-collecting optical system. However, as indicated in the appendix, the results given in Ref. 5 apply, strictly speaking, to the case where the number of modes collected by the imaging system are very large.

Specifically, γ is the cross-correlation function of the complex optical field before and after loading observed at a point in the observation plane, i.e., in practice at one resolution or pixel element in a detector array. Here we compute γ for three types of deformation, which for sufficiently small loadings will be independent: (1) tilt about an in-plane axis, (2) in-plane translations, and (3) a translation parallel to the optic axis. Here we assume an object is illuminated by a laser beam of mean wavevector $\underline{k}_i$. The scattered light of wavevector $\underline{k}_o$ along the optic axis propagates through a complex ABCD and the irradiance is recorded by a suitable detector array in the observation plane. It is assumed that the object is sufficiently rough such that the reflected light can be assumed to be spatially completely incoherent in the object plane. Specifically, we consider that the reflected light is given by $u(r) = \rho(r) \exp[i(\underline{k}_i - \underline{k}_o) \cdot \underline{r}]$, where $\rho(\underline{r})$ is the (complex)

reflection coefficient of the object. For an incoherent object radiating into a half space we have that $\langle \rho(r_1)\rho^*(r_2) \rangle = (2\pi/k^2) \, \delta(r_1 - r_2) I_s[(r_1 + r_2)/2]$, where k is the magnitude of the wavenumber, I_s is proportional to the brightness distribution of the source and is assumed here to be of the form $\exp[-2r^2/r_s^2]$, where r_s is the source spot radius.

3.1 In-Plane Tilt

In this situation, the reflected optical field after loading in an object plane transverse to the γ-axis is given by (assuming small tilt angles θ)

$$U_a(r) = \exp[ik\beta\theta r]U_b(r), \qquad (29$$

where $U_b(r)$ is the reflected field before loading,

$$\beta = (1 + \cos\alpha), \qquad (30)$$

and α is the angle between k_1 and the β-axis (i.e., the angle of incidence of the illumination beam).

The correlation function is obtained by employing Eq. (29) in Eq. (1) and substituting the resulting expressions into Eq. (28). The ensemble average is readilly obtained by noting that $\langle U_b(r_1)U_b^*(r_2) \rangle = (2\pi/k^2)I_s[(r_1 + r_2)/2] \, \delta(r_1 - r_2)$.

Assuming a Gaussian shaped source spot size, the resulting Gaussian integral can be integrated analytically. After a straight forward calculation, it can be shown that (assuming a tilt about the y-axis)

$$\gamma = |\gamma|e^{i\phi}t, \qquad (31)$$

21

where

$$|\gamma| = \exp[-\theta^2/\theta_t^2],$$ (32)

$$\theta_t = \frac{\rho_o}{2|B|\beta},$$ (33)

$$\phi_t = -\frac{4\beta \text{Im}(B)p_x\theta}{\rho_o^2}$$ (34)

ρ_o^2 is given by Eq. (12), B is the B-matrix element of the optical system before loading, and p_x is the projection of the observation coordinate vector onto the x-axis. Equations (31)-(34) give the load induced object tilt correlation coefficient for a complex ABCD optical system applicable to phase-shifting speckle interferometry. Note, for a point source (i.e., $r_s \rightarrow 0$, $\rho_o \rightarrow \infty$) we obtain, as expected intuitively, that $\gamma \rightarrow 1$.

3.2 In-Plane Translation

In this situation the load induces a uniform displacement of the object by an amount $\Delta\underline{r}_o$ perpendicular to the β-axis. Thus, the reflected object field after loading can be expressed as

$$U_\text{a}(\underline{r}) = U_\text{b}(\underline{r}-\Delta\underline{r})$$ (35)

By following the same procedure used in sec 3.1, it can be shown that the in-plane translation induced correlation coefficient is given by

$$\gamma = |\gamma|e^{i\phi}\exp[i(\underline{k}_i-\underline{k}_o) \cdot \Delta\underline{r}],$$ (36)

where

$$|\gamma| = \exp\left[-\frac{(\Delta r)^2}{r_d^2}\right], \tag{37}$$

$$r_d = \frac{\rho_o}{|A|}, \tag{38}$$

$$\phi = c_1 \Delta r^2 + c_2 \underline{\rho} \cdot \underline{\Delta r} \tag{39}$$

$$c_1 = \frac{4\text{Re}(BA^*)}{k r_s^2 \rho_o^2} \tag{40}$$

and

$$c_2 = k \, \text{Re}(1/B) - \frac{4\text{Im}(1/B)\text{Re}(BA^*)}{\rho_o^2} \tag{41}$$

Equation (35)-(41) gives the correlation coefficient for load induced in-plane translation for complex ABCD systems. For a point source ($r_2 \to 0$) on the optic axis we obtain that $|\gamma| = 1$, $c_1 = k \, \text{Re}(A/B)/2$, and $c_2 = k \, \text{Re}(1/B)$, which is identical to what one would obtain from Eq. (1) directly. As expected physically, the correlation coefficient for a point source is a pure phasor.

3.3 Translations parallel to the optic axes

When the load induces a translation along the z-axis by an amount Δz, the field after loading can be obtained from the corresponding field before loading by replacing the ABCD matrix elements by $\tilde{A}$, $\tilde{B}$, $\tilde{C}$, and $\tilde{D}$, where

23

$$\begin{bmatrix} \tilde{A} & \tilde{B} \\ \tilde{C} & \tilde{D} \end{bmatrix} = \begin{bmatrix} A & B \\ C & D \end{bmatrix} \begin{bmatrix} 1 & \Delta z \\ 0 & 1 \end{bmatrix}$$

That is, U_a is given by Eq. (1) with the matrix elements $(\tilde{A} \ \tilde{B} \ \tilde{C} \ \tilde{D})$, where $\tilde{A} = A$, $\tilde{B} = B + A\Delta z$, $\tilde{C} = C$, and $\tilde{D} = D + C\Delta z$.

Similarily, by following the same procedure outlined in sec 3.1, it can be shown that the correlation coefficient for translations along the optic axis is given by

$$\gamma = a \ \exp[i(\underline{k}_1 - \underline{k}_0)_z \Delta z] \ \exp[ik[Re(D/B) - Re(D/\tilde{B})]p^2/2] \ \exp[-c_3 \ p^2/\omega^2], \qquad (42)$$

where ω, the spot size in the observation plane before loading, is given by Eq. (13),

$$a = \frac{\rho_{oa}\rho_{ob}}{|\tilde{\rho}_o^2|}, \qquad (43)$$

$$\tilde{\rho}_o^2 = \rho_{oa}^2 + 2\Delta z \left[\frac{4AB^*}{(kr_s)^s} - i \ \frac{|A|^2}{k} \right], \qquad (44)$$

ρ_{oa} is given by Eq. 12, ρ_{ob} is obtained from Eq. (12) by replacing A and B by $\tilde{A}$ and $\tilde{B}$, respectively, and c_3 is a (complex) constant with $|c_3| \lesssim 1$, and $Re(c_3) \gtrless 0$. Although a rather lengthy expression for c_3 as a function of Δz and $A, .. D$ can be written down it is of no great concern here. This can be seen by recognizing that, in practice, meaningful information from the secondary fringe are obtained in the regime of the observation plane where the recorded intensity is relatively high (i.e., for $p \lesssim \omega$). Restricting our attention to values of p near the center of the spot (i.e., near $p = 0$), the

magnitude of the correlation coefficient for displacements parallel to the optic axis is equal to the amplitude coefficient a, given by Eq. (43). For a pointsource, $a \to 1$, the correlation coefficient is a pure phasor.

3.4 Applications

We now apply the results of secs 3.1-3.3 to three optical systems of concern to phase difference speckle interferometry and obtain analytic expression for the magnitude of the correlation coefficient $|\gamma|$. This quantity relates directly to fringe visibility (see Eqs. (15) and (17) of Ref. 5).

As indicated schematically in Fig. 2, the clean imaging optical system consists of a large positive thin lens of focal length f_1 placed a distance f_1 to the right of a Gaussian shaped source of radius r_s. At a distance f_1 to the right of this lens is a Gaussian shaped limiting aperture of radius σ. At a further distance f_2 to the right of this aperture is a large positive thin lens of focal length f_2. Finally, the observation plane is located a further distance f_2 to the right of this lens. An imaging system of this type is convenient since by varying the limiting aperture radius σ, one can match the target resolution to ensure a fully resolved speckle pattern across the detector array. Furthermore, since the limiting aperture is placed in the Fourier plane the clean imaging system is relatively insensitive to vignetting effects, and quadratic phase factors, present in direct imaging systems, are absent here leading to mathematical simplifications of the complex field in the observation plane.
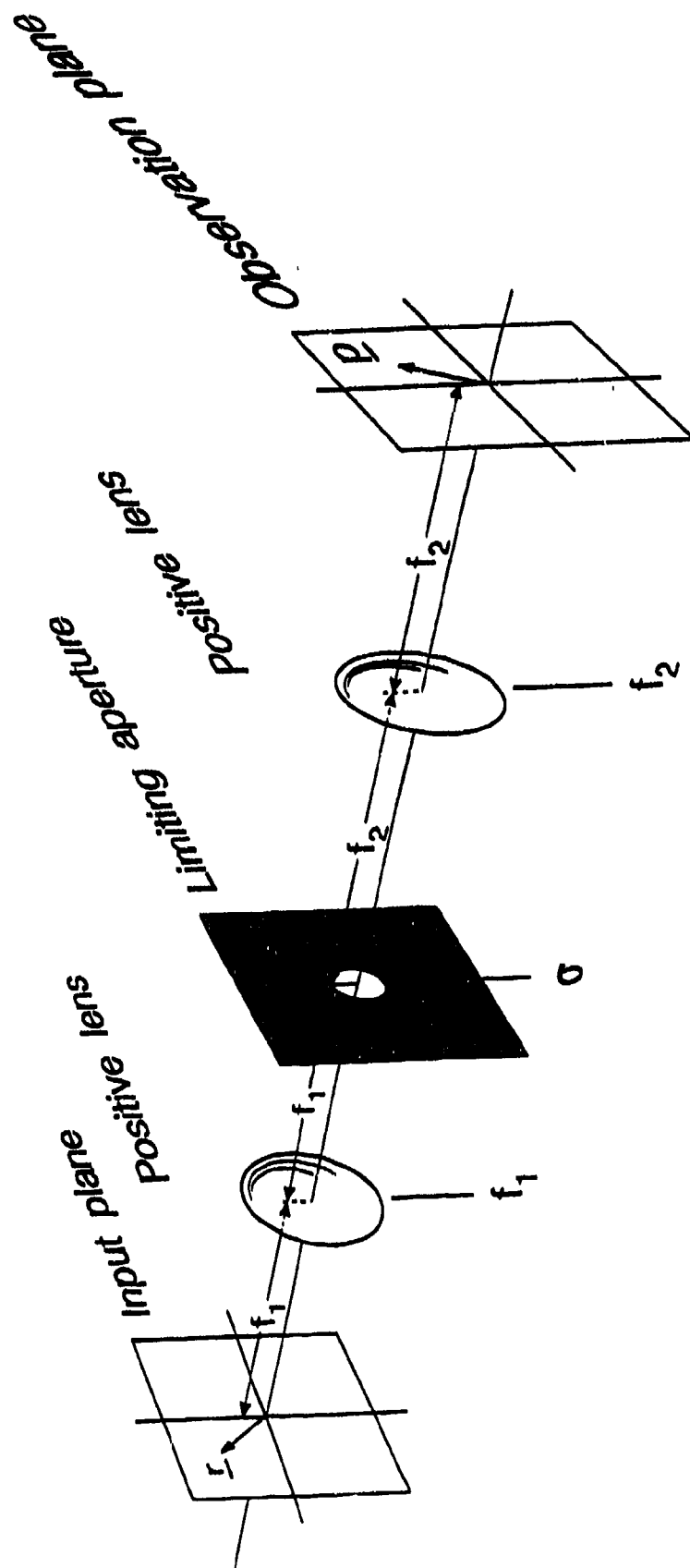
Figure 2. Schematic representation of a "clean" imaging optical system.

The appropriate ray matrix elements are given by: $A = f_2/f_1$, $B = 2if_1f_2/k\sigma^2$, and $D = f_1/f_2$. The mean speckle size ρ_0 and magnitude of the spot size ω are given by

$$\rho_0 = \left(\frac{2f_2}{k\sigma}\right)\left(\frac{2N}{N-1}\right)^{1/2} \tag{45}$$

$$\omega = \left(\frac{2f_2}{k\sigma}\right)N^{1/2} \tag{46}$$

where N, the number of modes "captured" by the system, takes the form

$$N = 1 + \left(\frac{k\sigma\, r_s}{2f_1}\right)^2 \tag{47}$$

Next consider a direct imaging system where a positive lens of focal length f and Gaussian radius σ is located a distance L_1 to the right of a source of radius r_s. At a further distance L_2, to the right of the lens (where $L_2^{-1} + L_1^{-1} = f^{-1}$) is the observation plane. The appropriate ABCD matrix elements are given by Eqs. (17) for $\sigma_a \to \infty$. It is easily seen that the quantities ρ_0, ω, and N are identical to those obtained above for the "clean" imaging system with $f_{1,2} \to L_{1,2}$.

Finally, we consider a Fourier transform optical system. Such a system may be of interest to measurement of surface rotation and tilt[8]. Tiziani shows that under these conditions the rigid body tilt is measured independently of any lateral displacement. The appropriate ray matrix elements are given by Eqs. (22) and we readily obtain from Eqs. (23) and (24) that

$$\rho_0 = \left(\frac{2f}{k\sigma}\right)\left(\frac{2N}{N-1}\right)^{1/2}\left[1 + \frac{(k\sigma^2/2f)^2}{N}\right]$$ (48)

and

$$\omega^2 = \left(\frac{2f}{k\sigma}\right)^2 N + \sigma^2,$$ (49)

where the number of modes N is given by Eq. (47).

In Table 1 we present the corresponding results for the correlation coefficients. For single mode systems (i.e., $N \rightarrow 1$, $\rho_0 \rightarrow \infty$) the correlation coefficient is unity and fringe visibility will be unaffected by load induced deformations. On the other hand, for direct imaging, and $N \gg 1$, the results presented in Table 1 for both the in-plane tilt and displacement agree qualitatively with the results of Ref. 5 for the case where the imaging lens is in the limit of Fresnel diffraction (i.e., $L_1 \ll k\sigma^2$).

To illustrate the effects on decorrelation due to finite N we consider clean imaging and plot the $|\gamma|$ as a function of both θ and Δr, normalized to the respective decorrelation parameter for $N \rightarrow \infty$. Since both θ_t and r_d depend on N in an identical manner we obtain a single family of curves, which are plotted in Fig. 3. Examination of Fig. 3 indicates that for $N \approx 10$, one may employ the decorrelation lengths for both tilt and in-plane displacement obtained for $N \rightarrow \infty$ with negligible error.

For local induced deformations along the optic axis, we see from Table 1 that $|\gamma|$ decorrelates with the characteristic length z_0 (where z_0 is of the order the depth of field) for the clean and direct imaging (for $L_1 \ll k\sigma^2$) and with the fresnel length $k\sigma^2$ for the Fourier transform system.
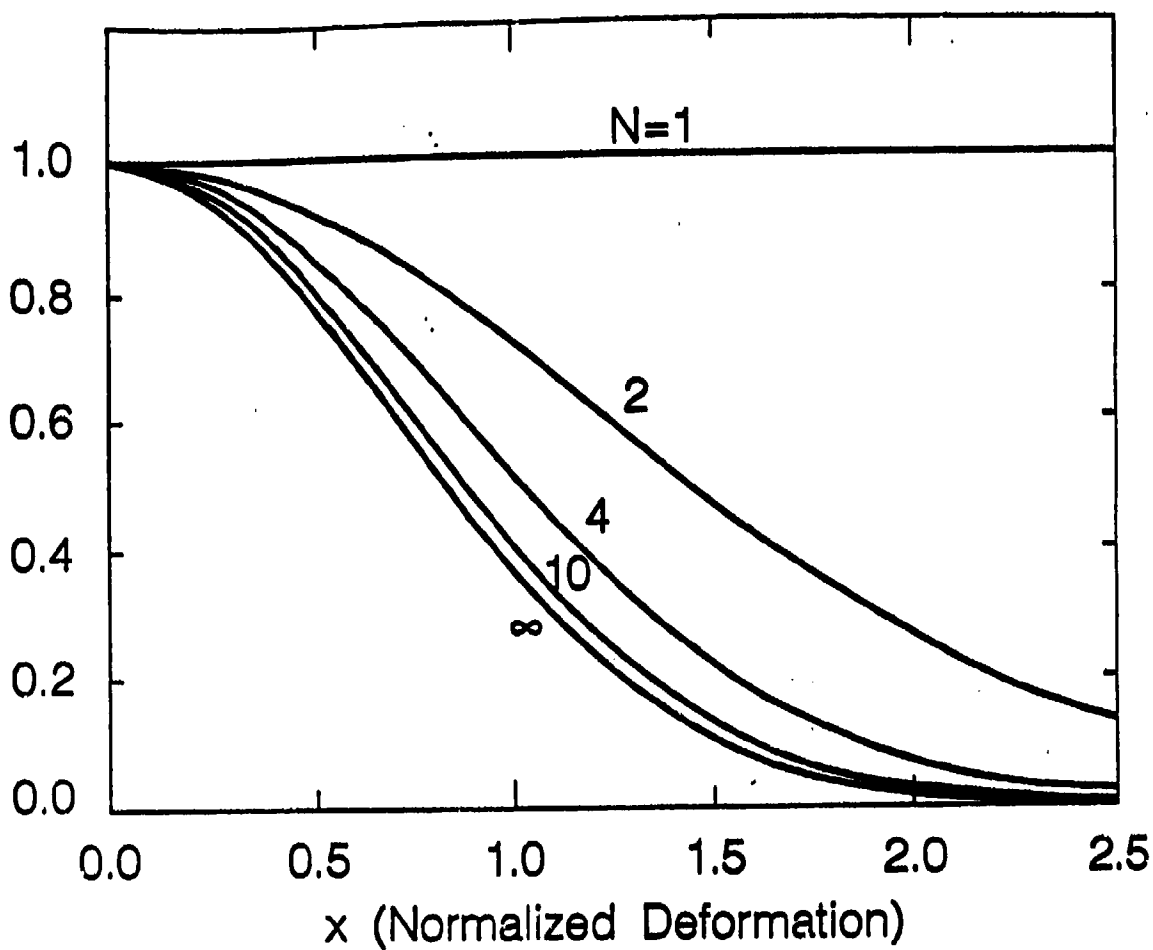
Figure 3. The magnitude of the correlation coefficient for imaging systems as a function of normalized deformations for various values of N. For in-plane tilt and in-plane displacement $x = \theta/\theta_{t\infty}$ and $\Delta r/r_{d\infty}$, respectively, where $\theta_{t\infty}$ and $r_{d\infty}$ are the respective decorrelation parameters in Table 1 for $N \rightarrow \infty$ (e.g., for the clean imaging system $\theta_{t\infty} = \sigma/\sqrt{2} \, f_1\beta$ and $r_{d\infty} = 2\sqrt{2} \, f_1/k\sigma$).

Table 1. The Magnitude of the Correlation Coefficient as a Function of the Number of Modes, N, for Three Types of Load-induced Deformations

System	Tilt: $|\tau| = exp\left(-\theta^2/\theta_t^2\right)$	In-Plane Displacement: $|\tau| = exp\left(-\Delta r^2/r_d^2\right)$	Displacement Parallel to the Optic Axis: $|\tau| = z$
Clean Imaging	$\theta_t = \dfrac{1}{\sqrt{2}}\left[\dfrac{\sigma}{f_1}\right]\left[\dfrac{N}{N-1}\right]^{1/2}\beta^{-1}$ where $\beta = 1 + \cos\alpha$	$r_d = \dfrac{2\sqrt{2}\,f_1}{k\sigma}\left[\dfrac{N}{N-1}\right]^{1/2}$	$z = \left\{\dfrac{1 + 4(\Delta z/z_e)^2/N}{1 + (\Delta z/z_e)^2\left(\dfrac{N+1}{N}\right)^2}\right\}^{1/2}\cdot$ where $z_e = 4f_1^2/k\sigma^2$
Direct Imaging	$\theta_t = \dfrac{1}{\sqrt{2}}\left[\dfrac{\sigma}{L_1}\right]\left[\dfrac{N}{N-1}\right]^{1/2}\beta^{-1}\cdot$	$r_d = \dfrac{2\sqrt{2}\,L_1}{k\sigma}\left[\dfrac{N}{N-1}\right]^{1/2}$ $\cdot\left[1 + (2L_1/k\sigma^2)^2\right]^{-1/2}$	$z = \left\{\dfrac{1 + 4(\Delta z/z_e)^2/N}{1 + \left(\dfrac{\Delta z}{z_e}\right)^2\left[\dfrac{N+1}{N}\right]^2 + \dfrac{N-1}{N}\left[\dfrac{2L_1}{k\sigma^2}\right]^2}\right\}^{1/2}$ where $z_e = 4L_1^2/k\sigma^2$
Fourier Transform	$\theta_t = \dfrac{1}{\sqrt{2}}\left[\dfrac{\sigma}{f}\right]\left[\dfrac{N}{N-1}\right]\beta^{-1}$ $\cdot\left[\dfrac{1 + (k\sigma^2/2f)^2/N}{1 + (k\sigma^2/2f)^2}\right]^{1/2}$	$r_d = \sqrt{2}\,\sigma\left(\dfrac{N}{N-1}\right)^{1/2}$ $\cdot\left[1 + (k\sigma^2/2f)^2/N\right]$	$z = \left\{1 + \left(\dfrac{N-1}{N}\right)^2\left[\dfrac{\Delta z/k\sigma^2}{1 + (k\sigma^2/2f)^2/N}\right]^2\right\}^{-1/2}$

30

In contrast to tilt in-plane displacement, $|\gamma|$ decorrelates much slower as a function of Δz and N. These features are illustrated in Fig. 4 where $|\gamma|$ is plotted as a function of $\Delta z/z_0$ and various values of N. In particular, for N=∞, one obtains a finite residual correlation tail equal to $2N^{1/2}/(N+1)$. These features are illustrated in Fig. 4 where $|\gamma|$ for a clean imaging system is plotted as a function of $\Delta z/z_0$, where $z_0 = 4f_1^2/k\sigma^2$ is the depth of field of the objective lens and various values of the number of modes. For finite N, decorrelation effects become important when $\Delta z > z_0$. As an example consider wavelengths in the visible or near ir and $\Delta z \sim 0.1$ mm. Hence, if $f_1/\sigma \gtrsim 10$ load induced deformations along the optic axis are manifest in phase difference interferometry. Such a situation may be obtained, for example, in a system that employs a microscope.

For the Fourier transform system the characteristic decorrelation length is given by $k\sigma^2$, the Rayleigh range of the Fourier transform lens. For practical applications $k\sigma^2$ is generally much greater than all load deformations Δz of interest and hence we conclude that Fourier transform systems will be insensitive to displacements along the optic axis in phase difference interferometry applications.
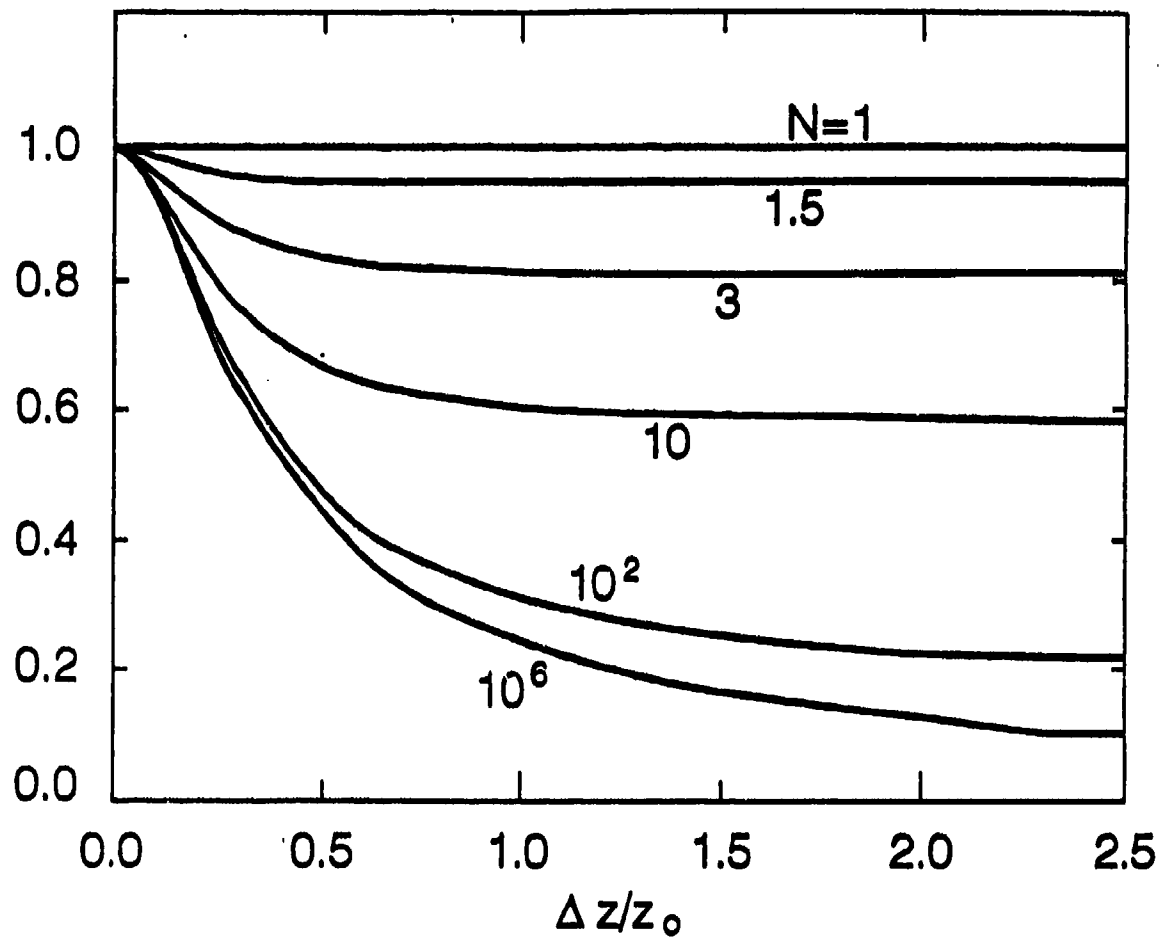
Figure 4. The magnitude of the correlation coefficient for a "clean" imaging system as a function of $\Delta z/z_0$ for various values of N, where Dz is the deformation along the z-axis and $z_0 = 4f_1^2 / k\sigma^2$ is the depth of field.

Appendix

Here we demonstrate that the results of Ref. 5 for the correlation function of the field are valid for $N \gg 1$, where N is the number of modes. Owner-Petersen considers a direct image-collecting geometry where a lens of diameter D collects light reflected of an object of amplitude reflection coefficient $\rho(\underline{r})$. Central to the derivation of the correlation function in Ref. 5 is the quantity A_ρ which is obtained in the calculation of the wavefront in the pupil plane. This quantity is the Fourier transform of ρ and in the notation employed here is given by

$$A_\rho(\underline{q}) = \int d^2 r \, \rho(\underline{r}) \, e^{i \underline{q} \cdot \underline{r}}, \tag{A-1}$$

where

$$\underline{q} = \frac{k \underline{r}_p}{L}, \tag{A-2}$$

L is the distance between the object and the lens, and $\underline{r}_p$ is a two-dimensional coordinate vector in the pupil plane [5]. In computing the correlation function Owner-Petersen asserts, in Eq. A10 of Ref. 5 that A_ρ is delta correlated:

$$\langle A_\rho(\underline{q}_1) \, A_\rho^*(\underline{q}_2) \rangle = \text{constant } \delta(\underline{q}_1 - \underline{q}_2) \tag{A-3}$$

To see under what condition this is valid we have from Eq. A-1 that

$$\langle A_\rho(\underline{q}_1) \, A_\rho^*(\underline{q}_2) \rangle = \int d^2 r_1 \int d^2 r_2 \, \langle \rho(\underline{r}_1) \, \rho^*(\underline{r}_2) \rangle \, e^{i(\underline{q}_1 \cdot \underline{r}_1 - \underline{q}_2 \cdot \underline{r}_2)} \tag{A-4}$$

For a completely incoherent source the phase of ρ is random with statistics $\langle \rho(\underline{r}_1)\rho^*(\underline{r}_2) \rangle = \text{constant } \delta(\underline{r}_1 - \underline{r}_2)$. Using this into Eq. (A-4) yields

$$\langle A_\rho(\underline{q}_1) \, A_\rho^*(\underline{q}_2) \rangle = \text{constant} \int d^2 r |\rho(\underline{r})|^2 \, e^{i(\underline{q}_1 - \underline{q}_2) \cdot \underline{r}} \tag{A-5}$$

Now in order that the right hand side of Eq. A-5 resemble a delta function it is necessary for the exponential term in the integral to undergo many oscillations for $q_1 = q_2$. This condition will be satisfied if $|\rho|$ is slowly varying and

$$|(\underline{q}_1 - \underline{q}_2) \cdot \underline{r}|_{max} \sim \frac{kDr_s}{L} \gg 1, \qquad \text{(A-6)}$$

where r_s is of the order the size of the object. Comparing Eg. A-6 with Eq. 47 indicates that Eq. A-6 is equivalent to the condition that the number of modes $N \gg 1$.

Indeed, Eq. A-6 can be obtained by an elementary argument. Physically, one can consider the optical field in the pupil plane to be delta correlated when the lateral coherence length of the field is much less than the pupil diameter D. By the van-Cittert Zernike theorem, the coherence length of an incoherent radiator of size r_s is of the order $\lambda r_s / L$, where λ is the optical wavelength. The condition that this coherence length is much less than D is identical to Eq. A-6. For many application Eq. A-6 is not satisfied and the assumption that A_ρ is delta correlated is not valid.

Reference

1. A.E. Siegman, "Lasers", University Science Books, Mill Valley CA., 1986.

2. H.T. Yura and S.G. Hanson, "Optical Beam Wave Propagation through Complex Optical Systems", J. Opt. Soc. Am. A, 4, 1931-1948 (1987).

3. H.T. Yura and S.G. Hanson, "Second-Order Statistics for Wave Propagation Through Complex Optical Systems", J. Opt. Soc. Am. A, 4, 564-575 (1989).

4. K. Creath, "Phaseshifting Speckle Interferometry", in International Conference on Speckle, H.H. Arsenault, ed., Proc. Soc. Photo-Opt. Instrum. Eng. 556, 337-346 (1985).

5. M. Owner-Petersen, "Decorrelation and Fringe Visibility: on the Limiting Behaviour of Various Electronic Speckle-Pattern Correlation Interferometers", Jr. Opt. Soc. Am. A, 8, 1082-1089 (1991).

6. J.W. Goodman, "Laser Speckle and Related Phenomenon", Vol. 9 of Topicsin Applied Physics, Springer-Verlag, Berlin, 1975.

7. M. Born and E. Wolf, "Principles of Optics", Pergamon Press, Oxford, 1975.

8. H. Tiziani: Opt. Commun. 5, 271 (1972).

TECHNOLOGY OPERATIONS

The Aerospace Corporation functions as an "architect-engineer" for national security programs, specializing in advanced military space systems. The Corporation's Technology Operations supports the effective and timely development and operation of national security systems through scientific research and the application of advanced technology. Vital to the success of the Corporation is the technical staff's wide-ranging expertise and its ability to stay abreast of new technological developments and program support issues associated with rapidly evolving space systems. Contributing capabilities are provided by these individual Technology Centers:

Electronics Technology Center: Microelectronics, solid-state device physics, VLSI reliability, compound semiconductors, radiation hardening, data storage technologies, infrared detector devices and testing; electro-optics, quantum electronics, solid-state lasers, optical propagation and communications; cw and pulsed chemical laser development, optical resonators, beam control, atmospheric propagation, and laser effects and countermeasures; atomic frequency standards, applied laser spectroscopy, laser chemistry, laser optoelectronics, phase conjugation and coherent imaging, solar cell physics, battery electrochemistry, battery testing and evaluation.

Mechanics and Materials Technology Center: Evaluation and characterization of new materials: metals, alloys, ceramics, polymers and their composites, and new forms of carbon; development and analysis of thin films and deposition techniques; nondestructive evaluation, component failure analysis and reliability; fracture mechanics and stress corrosion; development and evaluation of hardened components; analysis and evaluation of materials at cryogenic and elevated temperatures; launch vehicle and reentry fluid mechanics, heat transfer and flight dynamics; chemical and electric propulsion; spacecraft structural mechanics, spacecraft survivability and vulnerability assessment; contamination, thermal and structural control; high temperature thermomechanics, gas kinetics and radiation; lubrication and surface phenomena.

Space and Environment Technology Center: Magnetospheric, auroral and cosmic ray physics, wave-particle interactions, magnetospheric plasma waves; atmospheric and ionospheric physics, density and composition of the upper atmosphere, remote sensing using atmospheric radiation; solar physics, infrared astronomy, infrared signature analysis; effects of solar activity, magnetic storms and nuclear explosions on the earth's atmosphere, ionosphere and magnetosphere; effects of electromagnetic and particulate radiations on space systems; space instrumentation; propellant chemistry, chemical dynamics, environmental chemistry, trace detection; atmospheric chemical reactions, atmospheric optics, light scattering, state-specific chemical reactions and radiative signatures of missile plumes, and sensor out-of-field-of-view rejection.